A checkerboard pattern manifested by the oviduct epithelium of the Japanese quail

HACHIRO I. YAMANAKA* and HISAO HONDA

Kanebo Institute for Cancer Research, Osaka, Japan

ABSTRACT   The oviduct epithelium of the Japanese quail is a monolayered epithelium consisting of two types of columnar cells, goblet type gland (G-) cells and ciliated (C-) cells. We found these cells to be arranged in a checkerboard pattern. Three types of cell boundaries formed between the two different types of cells were examined statistically at various levels of the columnar cells. There was a tendency on the part of the cells to form boundaries between G- and C- cells rather than between two C- cells or between two G- cells. We therefore propose that the pattern is constructed under a rule of maximizing the length of boundaries of two different types of cells owing to the fact that theirs is the greatest adhesion capacity. The role of microfilament bundles running along the apical cell boundaries is also discussed. It is suggested that they are in a tense state so as to shorten total length by contraction.

KEY WORDS: *pattern formation, monolayered epithelium, cell adhesion property, microfilament bundles, boundary contraction*

Introduction

A monolayered epithelium is the simplest arrangement of cells seen in various animal tissues. It is a favorable situation in which to study mechanisms of morphogenesis because its structure can simply be regarded as a two-dimensional cell sheet. A monolayered epithelium, which consists of a single type of cell, shows a polygonal cellular pattern resembling a honeycomb (Owaribe et al., 1981; Honda, 1983). The honeycomb pattern is the pattern that makes the total cell boundaries shortest when cells are aligned on a plane without any gaps. It is thought that contraction of microfilament bundles along cell boundaries at the apical surface (Owaribe et al., 1981; Burgess, 1982; Owaribe and Masuda, 1982) is responsible for bringing about the honeycomb pattern (Eguchi, 1977; Honda and Eguchi, 1980; Honda 1983).

On the other hand, it is known that when cells of different types are mixed they can sort themselves out into a variety of patterns (Townes and Holtfreter 1955; Moscona 1956). This phenomenon is explained by the different adhesion capacities of various tissue cells, and is thought to have an important role in tissue morphogenesis in embryogenesis (Steinberg 1962a, b, c; 1978).

We are interested in monolayered epithelia consisting of two different types of cells where both mechanisms (contraction of cell boundaries and differential cell adhesion) are expected to be at work. The oviduct epithelium of the Japanese quail is suitable material for this purpose because the albumen-secreting region of

the tissue is a monolayered epithelium consisting of ciliated (C-) cells and goblet type gland (G-) cells (Romanoff and Romanoff, 1949; Hodges, 1974). These cells cover the luminal surface of the oviduct and help in the transport of ova by beating cilia and secreting mucin. respectively (Hodges, 1974). Although it is known that these two different types of cell alternate when viewed in vertical section (Hodges, 1974) the overall pattern has remained hidden due to the great number of obscuring cilia (Blom, 1973; Rumery and Eddy, 1973; Bakst, 1978).

In this paper, we analyze the pattern of boundaries between cells of the quail oviduct epithelium to learn more of the possible role of cell cohesion in pattern formation. The role of microfilament bundles at the apical surface region is also discussed.

Results

The pattern at the apical level

An oviduct epithelium stained with the silver impregnation method shows a checkerboard-like alignment of cells in many places (Fig. 1). This pattern consists of square C-cells and octagonal G-cells having four long G-C boundaries (those between G- and C-cells) and four short G-G boundaries (those between two G-cells) (Fig. 1b).

Although the silver impregnation is a convenient method for specific staining of the boundaries at the apical level, it cannot easily distinguish between two different types of cell. To make this

*Address for reprints: Kanebo Institute for Cancer Research, Pharmaceutical Division, Kanebo Ltd., 5-90 Tomobuchi-cho 1-chome, Miyakojima-ku, Osaka 534, JAPAN. FAX: 6-921.3883
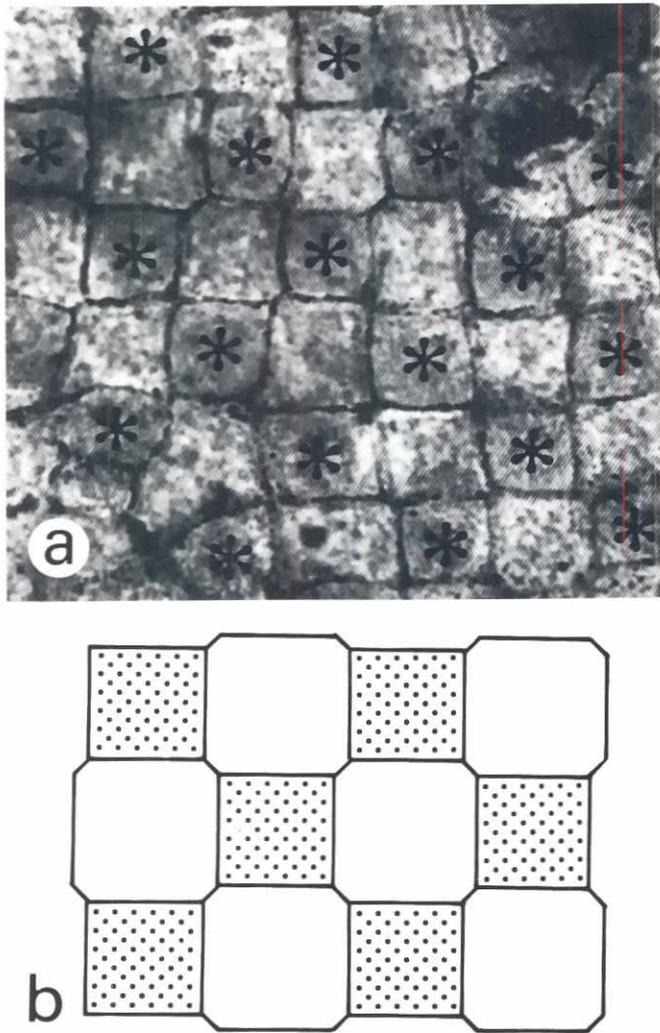
Fig. 1. A typical checkerboard pattern at the surface of the oviduct epithelium stained by silver impregnation. (a) *Cells identified as C-cells are indicated by asterisks. Short G-G boundaries are often observed, while C-C boundaries are scarcely seen. Location of silver granules at the apical cell boundaries of columnar cells was confirmed by changing the focal plane.* (b) *Schematic illustration of (a). Bar indicates 5 μm.*

Elsewhere a strict checkerboard pattern is not always observed because the ratio of G-cells to C- cells was an average of 1.29:1 (Table 1).

Constitution of cell boundaries at the apical level

The probabilities of obtaining each of the three types of boundaries constructed between two types of cells on a two-dimensional plane can be calculated from a binomial distribution, assuming a random distribution of the cells. When the ratio of G-cells to C-cells is 1.29 it is expected that 49.2%, 31.7% and 19.1% of the boundary should be G-C, G-G and C-C, respectively (see *2 in Table 4). As shown in Table 2, the actual frequency of G-C boundaries was higher, at 68.7%, while G-G and C-C boundaries were reduced to
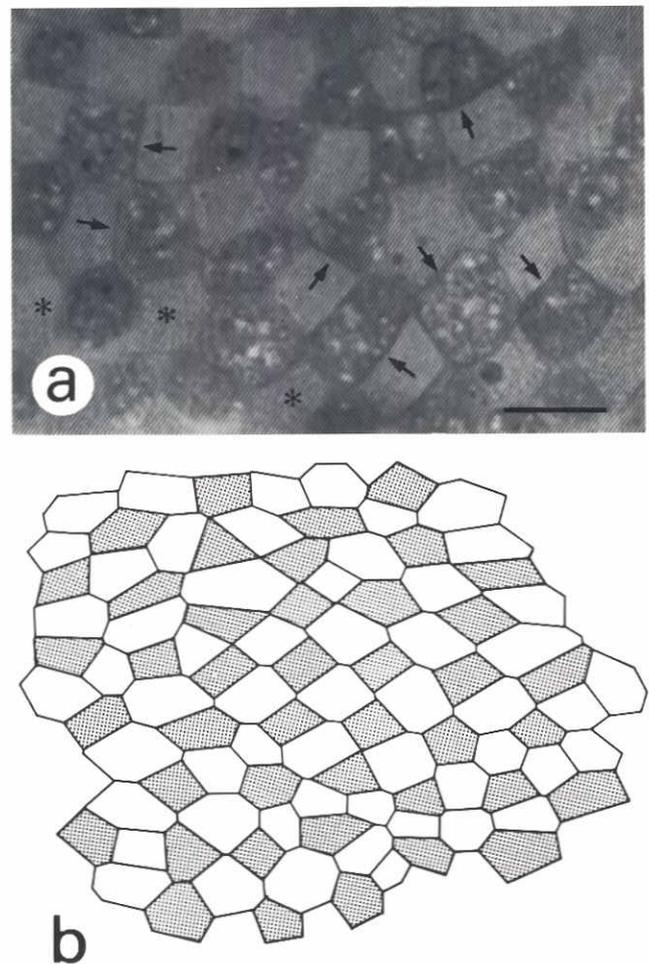
Fig. 2. Surface cellular pattern analyzed in this study. (a) *One of the serial 1 μm-thick sections cut tangential to the epithelial surface prepared from resin-embedded tissue. C-cells are identified by their numerous cilia (asterisks). G-cells appearing darker are easily distinguished from the C-cells by metachromasia of toluidine blue. Boundaries at the surface of the epithelium can be identified easily as thick lines in the photograph (arrows).* (b) *One of the three cellular patterns at the surface of the epithelium used for geometrical analyses. The patterns were prepared by superposing photographs of serial sections as shown in Fig. 2b. Open and shaded polygons indicate G- and C-cells, respectively. Bar in (a) indicates 10 μm.*

distinction, serial sections 1μm thick were cut tangential to the epithelial surface and stained with toluidine blue. One such section is shown in Fig. 2a. G-cells, which are stained darkly due to accumulated mucin, and C-cells which are stained lightly, are easily distinguishable. Boundaries at the apical level can be identified as straight, dense lines (arrows) while those at other levels are more indistinct and winding. Several neighboring sections were superimposed on each other so as to obtain a pattern consisting of straight and dense lines throughout. Thus we obtained three patterns from different regions, which were used for statistical analyses as described below. One such pattern is shown in Fig. 2b.

Population of two types of cells

The checkerboard pattern is observed in the central region of Fig. 2b, where locally the number of each type of cell is the same.

RATIO OF THE TWO TYPES OF CELLS IN OVIDUCT EPITHELIUM

	Region			
	a	b	c	Total
Cells				
G-cell	61	56	21	138
C-cell	45	44	18	108
G/C*	1.36	1.27	1.17	1.29

*Ratio of G-cells to C-cells

28.1% and 3.2%, respectively. The G-C boundary was also longer than expected, at 81.1% of the total length, whereas G-G and C-C boundaries were correspondingly reduced to 18.1% and 0.9%, respectively. The results mean that the G-C boundary occurs more frequently than by chance and is longer than expected. On the other hand G-G and C-C boundaries are less frequent and shorter.

Boundaries at subsurface level

The boundaries were compared between the apical and subsurface levels in the same cells. The boundaries under the surface level were sinuous (Fig. 3b) and not lined with filamentous structures as observed at the apical surface in Fig. 3a. The boundaries are illustrated in Fig. 3a' and 3b', where reduction of the G-G boundary is conspicuous. The total length of each boundary was estimated by measuring boundaries around ten C-cells and thirteen G- cells randomly picked from electron micrographs as shown in Fig. 3b. The G-C boundary was found to be highly extended, constituting 94.8% of the total length, while the G-G boundary was almost excluded (2.6%). The exclusively high amount of the G-C boundary was consistently observed from the subsurface to the basal level.

Filaments at the apical cell boundaries

The filamentous material lining the boundaries at the apical level was characterized. Electron micrographs of tangential sections of cells treated with digitonin showed the component filaments to be 6-7 nm thick (Fig. 4a, b). Fluorescent microscopy using antiactin antibody showed strong fluorescence along the cell boundaries (Fig. 4c). This fluorescence was confined to the apical level as confirmed by changing the focal plane. Thus, the dense filamentous material

TABLE 2

PERCENT RATIO OF THREE TYPES OF CELL BOUNDARIES AT THE APICAL SURFACE LEVEL OF OVIDUCT EPITHELIUM

		Region			
		a	b	c	Mean
Boundaries					
G-C	Number	68.5	67.5	71.1	68.7
	Length	79.1	80.1	87.7	81.1
G-G	Number	27.7	30.3	23.7	28.1
	Length	20.1	19.4	10.4	18.1
C-C	Number	3.8	2.1	4.4	3.2
	Length	0.7	0.6	1.8	0.9

consists of a bundle of actin filaments running along the boundaries at the apical level circumferentially in both types of cells.

Discussion

We found a unique alternating cell arrangement in the oviduct epithelium of the Japanese quail. It often shows a checkerboard pattern where cells are present in equal proportions. We showed that the frequency and length of G-C boundaries were greater than those expected on the assumption of a random distribution of the two types of cells. Therefore, we propose that the stronger adhesion between G- and C-cells compared to G-G or C-C cell adhesion is a principal factor in the tissue's morphogenesis. In other words, the checkerboard pattern is spontaneously brought about by the tendency of the G-C boundaries to enlarge. The G-G boundary, which is one of the boundaries between like cells, was shown to be 20-30%

TABLE 3

LENGTH OF CELL BOUNDARIES AT THE SUBSURFACE LEVEL

Type of boundary	Length of boundary* (μm)	Ratio (%)
G-C	1438.5	94.8
G-G	40.0	2.6
C-C	39.2	2.6

* Boundary length was obtained by measuring thirteen G-cells and ten C-cells in the electron micrographs of tangential sections.

of the total in frequency and length while the C-C boundary was almost excluded. We propose the adhesion intensities of these cell borders to be in the sequence: G-C >G-G >>C-C.

In a three-dimensional cell mass where two types of cells have been artificially mixed, the cells are expected to arrange themselves in various patterns as a function of the differences in their mutual adhesiveness (Steinberg 1962c, 1978). When "cross-adhesions" (between two unlike cell types) are weaker than the average of the adhesions between the two like kinds of cells, the unlike cells are expected to sort out from one another. The precise configuration adopted is a function of the relative adhesive intensities involved. If cross-adhesions are of intermediate strength, the more weakly cohering cell population should completely envelop the more strongly cohering population. On the other hand, if cross adhesions are the weakest kind, the above envelopment should be partial rather than complete. Finally, when "cross-adhesions" are stronger than the average of the adhesions between the two like kinds of cells, the unlike cells are expected to intermix rather than sort out (Steinberg 1962c, 1978), with unlike cells alternating (Goel et al., 1975). However, no actual instance of the intermixing case had been found so far. The situation in the quail oviduct epithelium is considered to be equivalent to the intermixing case but in a two-dimensional cell sheet.

Boundaries at the apical surface level of epithelial cells are lined with actin filament bundles. These types of boundaries have been shown to be in a state of tension and to form a honeycomb pattern in cell sheets of a homogeneous cell population (Honda and Eguchi 1980; Owaribe et al., 1981; Owaribe and Masuda 1982). This
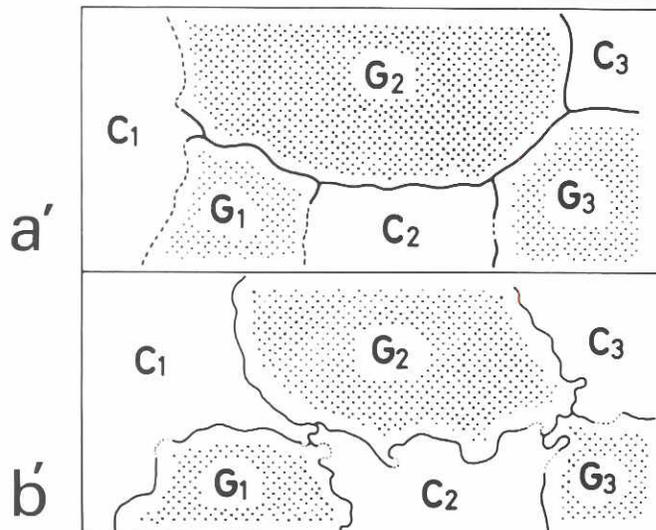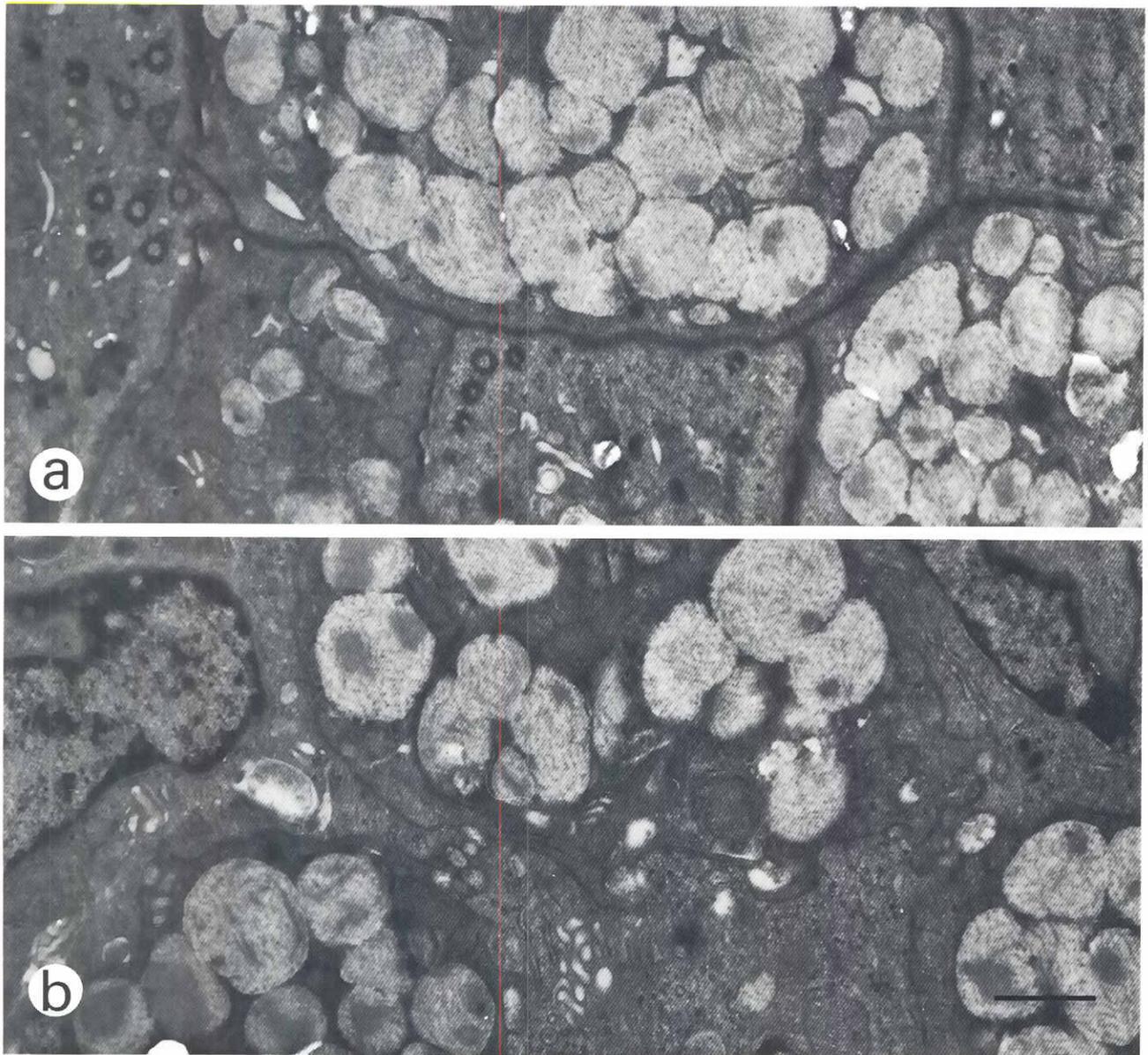
Fig. 3. Electron micrographs of tangential sections of the columnar epithelial cells at two different levels. Three C-cells (C1, C2, C3) and three G-cells (G1, G2, G3) are identified. (a) *Apical surface level. The circumferential microfilament bundles can be observed along cell boundaries.* (b) *Subsurface level. Boundaries are winding and not decorated as in (a).* (a') *and* (b') *drawings showing cell boundaries of photographs (a) and (b). Bar 1 µm.*
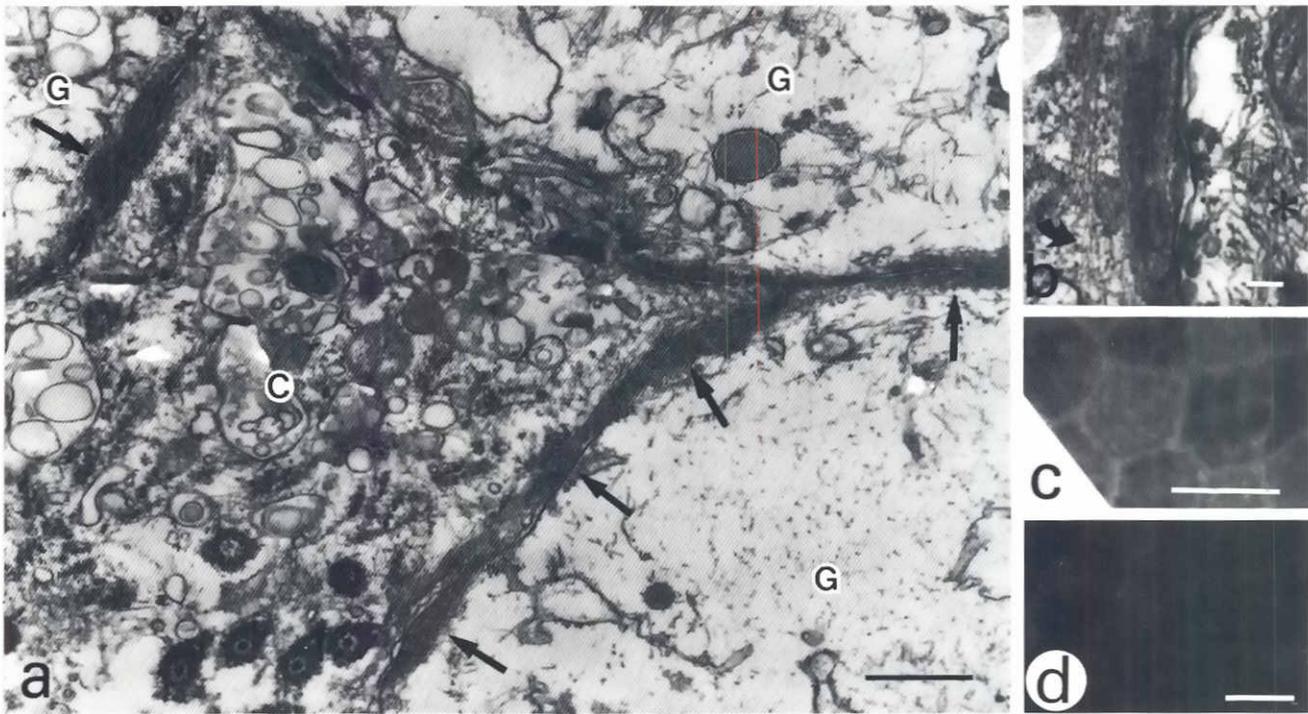
Fig. 4. Electron micrographs of cell boundaries at the surface of the epithelium. *The specimen was treated with digitonin and tannic acid as described in Materials and Methods.* **(a)** *Bundles of microfilaments are observed along the cell boundaries both in the C-cells (C) and the G-cells (G).* **(b)** *Same as (a) at a higher magnification. Microfilaments, which can be easily distinguished from intermediate filaments (asterisks), run parallel to the cell boundary (arrows) and constitute the circumferential microfilament bundles.* **(c)** *Immunofluorescence micrographs of the oviduct epithelium stained with antibody to actin.* **(d)** *Control of (c) at lower magnification. C-cells show slight nonspecific fluorescence in their cytoplasm but are clearly distinct from specific fluorescence in (c). Bars in (a), (b), (c) and (d) are 1µm, 0.1µm, 10µm and 1µm respectively.*

tension which is an opposing force to the formation of the checkerboard pattern, should also act at the apical surface of this tissue. The straight appearance of apical boundaries compared to that at other levels suggests the presence of tension along the boundary.

The fact that the apical surface polygonal pattern is scarcely affected by hypertrophy of G-cells while that of other levels is seriously distorted (Hodges, 1974) also indicates the presence of tension.
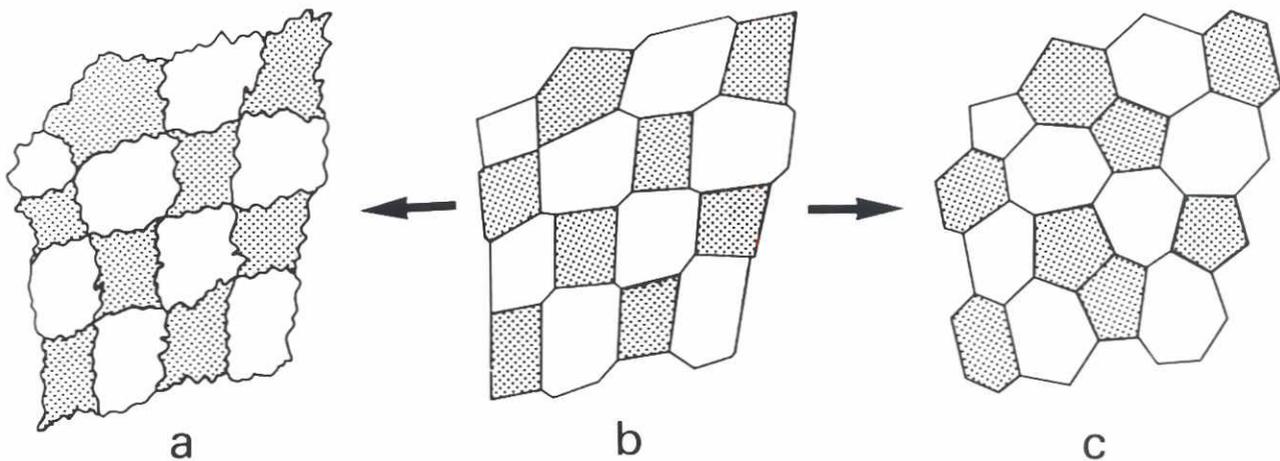
Fig. 5. Contribution of the two factors, contraction of cell boundaries and differential cell adhesion, to the surface cellular pattern. *Open and shaded polygons are the G- and C-cells respectively.* **(b)** *Actual pattern at the apical surface level (a part of Fig. 2b).* **(a)** *A pattern schematically drawn for the pattern at the subsurface level of (b).* **(c)** *A pattern whose total cell boundary length was shortened by the boundary contraction procedure from the pattern (b).*

TABLE 4

LENGTH CONSTITUTION OF THE THREE TYPES OF CELL
BOUNDARIES IN PATTERNS SHOWN IN FIG. 5

Boundaries	*1	a	b	c	*2
G-C	100	94.8	81.1	68.6	49.2
G-G	0	2.6	18.1	25.8	31.7
C-C	0	2.6	0.9	5.6	19.1

a-c, corresponding to the designations in Fig. 5. a, the actual values shown in Table 3 for the subsurface pattern.
b,   actual values for surface pattern shown in Table 2.
c,   values measured after the boundary contraction procedure.
*1, value for a geometrical checkerboard pattern.
*2, values for the chance of neighboring, normalized to 100. Probabilities of the neighboring of a G-cell and C-cell, two G-cells and two C-cells are $2N_G \times N_C$, $N_G \times N_G$ and $N_C \times N_C$, respectively, where N_G and N_C are the populations of the G-cells and C-cells whose ratio is 1.29 as shown in Table 1.

The curtailed cell boundaries are considered to have physiological advantages by saving the total amount of materials of the junctional complex and reducing the risk of breakage in its sealing function.

We speculated that the contractile activity of microfilament bundles working at the apical level shifts the checkerboard pattern to the honeycomb pattern to some extent. This results in the appearance of the G-G boundary because G-cells are thought to have the second strongest adhesion capacity. To support this idea, Fig. 5b (a part of Fig. 2b) was processed according to the factors mentioned above. The pattern at the subsurface level was concluded to be influenced only by the adhesion property, because of the lack of actin bundles and the winding appearance of the boundary (Fig. 5a). In fact, the length ration of the G-C boundary became almost (94.8% in Table 4, column a) that of an ideal checkerboard pattern (100%) (Table 4 column *1). On the other hand, the pattern produced from Fig. 5b after the boundary contraction procedure is that of Fig. 5c. The values for each boundary approached those of a regular honeycomb pattern (Table 4 *2). In this case, the difference of G-G, C-C and G-C boundary adhesion properties is completely omitted.

Materials and Methods

Quail oviduct

Japanese quails (*Coturnix coturnix japonica*) were purchased from Nihon-Uzura Co. Ltd. (Toyohashi, Japan), and kept in our laboratory (Honda et al., 1982b). The thickest part of albumen-secreting region of the oviduct was used for all experiments. The oviduct was obtained when a ovum had just passed through the region, that is 2 to 3 hr after laying, as the cellular pattern of the epithelium is distorted by hypertrophy of G-cells due to accumulation of mucin prior to the passage of an ovum (Hodges, 1974).

Staining of cell boundaries by silver impregnation

The inner surface of the oviduct was exposed by a surgical cut, rinsed with distilled water and dipped into more than 20 volumes of 0.5% silver nitrate solution with 2% nitric acid for 5 min at room temperature. The tissue was washed with distilled water and developed by exposure to white light in 1%

hydroquinone for 30 min. The oviduct epithelium was peeled off with forceps, mounted on slides with glycerol, observed and photographed with a light microscope (Leitz Orthoplan).

Light and electron microscopy of resin-embedded tissues

The oviduct was fixed and processed routinely (Yamanaka and Eguchi, 1981). Eight to ten serial sections of 1μm thickness were cut tangentially to the epithelial surface, mounted on a cover glass, stained with toluidine blue, and observed with a light microscope. Ultra-thin sections were also prepared and inspected with a JEOL 100-C electron microscope after staining with uranyl acetate and lead citrate. To study the circumferential microfilament bundles, the oviduct was pretreated with 0.1 mg/ml of soluble digitonin (Bridges, 1977) in Dulbecco's phosphate buffered saline (PBS), and fixed primarily with 2% glutaraldehyde in sodium cacodylate buffer supplemented with 0.2% tannic acid.

Immunofluorescence microscopy

An antibody prepared against *Physalium polycephalum* actin was obtained from Dr. K. Owaribe of Nagoya University (Owaribe and Hatano, 1975; Owaribe et al., 1979). FITC-conjugated sheep antibody to rabbit IgG was from Miles Laboratories Ltd. (Elkhart, IN, USA). The oviduct was fixed with 10% neutral formalin and the epithelium was peeled off. The tissue was incubated with anti-actin antibody or with non-immune rabbit IgG for 40 min at 37°C. After washing with PBS the tissue was stained with FITC-conjugated anti-rabbit IgG, and observed with an incident light fluorescence microscope (Leitz Orthoplan).

The boundary contraction procedure

A geometrical procedure was developed for simulating patterns comprised of convex polygons covering a plane without gaps or overlaps (Honda and Eguchi, 1980; Honda et al., 1982a). With the aid of a digital electronic computer, an observed pattern is transformed into one whose total side length is shorter than the original, but with the area of the polygons being kept constant.

References

BASKST, M.R. (1978). Scanning electron microscopy of the oviductal mucosa apposing the hen ovum. *Poultry Sci. 57:* 1065-1069.

BLOM, L. (1973). Ridge pattern and surface ultrastructure of the oviductal mucosa of the hen *(Gallus domesticus)*. *Biol. Skr. Dan. Vid. Sel. 20:* 1-41.

BRIDGES, C.D.B. (1977). A method for preparing stable digitonin solutions for visual pigment extraction. *Vision Res. 17:* 301-302.

BURGESS, D.R. (1982). Reactivation of intestinal epithelial cell brush border motility: ATP-dependent contraction via a terminal web contractile ring. *J. Cell Biol. 95:* 853-863.

EGUCHI, G. (1977). Cell shape changes and establishment of tissue structure. *Saiensu* (Japanese edition of *Scientific American*) 7 (5): 66-77.

GOEL, N., CAMPBELL, R.D., GORDON, R., ROSEN, R., MARTINEZ, H. and YCAS, M. (1975). Self sorting of isotropic cells. In *Mathematical Models for Cell Rearrangement* (Ed. G.D. Mostow). Yale Univ. Press, New Haven, London, pp. 100-144.

HODGES, R.D. (1974). *The Histology of the Fowl.* Acad. Press Co., London.

HONDA, H. (1983). Geometrical models for cells in tissues. *Int. Rev. Cytol. 81:* 191-248.

HONDA, H. and EGUCHI, G. (1980). How much does the cell boundary contract in a monolayered cell sheet? *J. Theor. Biol. 84:* 575-588.

HONDA, H., OGITA, Y., HIGUCHI, S. and KANI, K. (1982a). Cell movements in a living mammalian tissue: long term observation of individual cells in wounded corneal endothelia of cats. *J. Morphol. 174:* 25-39.

HONDA, H., TANAKA, K., MINAMINO, T. and KONISHI, T. (1982b). Control of contour feather growth of Japanese quail. *J. Exp. Zool. 220:* 311-319.

MOSCONA, A. (1956). Development of heterotypic combination of dissociated embryonic chick cells. *Proc. Soc. Exp. Biol. Med. 92:* 410-416.

OWARIBE, K. and HATANO, S. (1975). Introduction of antibody against actin from myxomycete plasmodium and its properties. *Biochemistry 14:* 3024-3029.

OWARIBE, K., IZUTU, K. and HATANO, S. (1979). Cross-reactivity of antibody to physalum actin and actins in eukaryotic cells examined by immunofluorescence. *Cell Struct. Funct. 4:* 117-126.

OWARIBE, K., KODAMA, R. and EGUCHI, G. (1981). Demostration of contractility of circumferential actin bundles and its morphogenetic significance in pigmented epithelium *in vitro* and *in vivo. J. Cell Biol. 90:* 507-514.

OWARIBE, K. and MASUDA, H. (1982). Isolation and characterization of circumferential microfilament bundles from retinal pigmented epithelial cells. *J. Cell Biol. 95:* 310-315.

ROMANOFF, A.F. and ROMANOFF, A.J. (1949). *The Avian Egg.* John Wiley and Sons, Inc., New York.

RUMERY, R.E. and EDDY, E.M. (1973). Scanning electron microscopy of the fimbriae and ampullae of rabbit oviducts. *Anat. Rec. 178:* 83-102.

STEINBERG, M.S. (1962a). On the mechanism of tissue reconstruction by dissociated cells. I. Population kinetics, differential adhesiveness, and the absence of direct migration. *Proc. Natl. Acad. Sci. USA 48:* 1577-1582.

STEINBERG, M.S. (1962b). Mechanisms of tissue reconstruction by dissociated cells. II. Time course of events. *Science 137:* 762-763.

STEINBERG, M.S. (1962c). On the mechanism of tissue construction by dissociated cells. III. Free energy relations and the reorganization of fused heteronomic tissue fragments. Proc. Natl. Acad. Sci. USA 48: 1769-1776.

STEINBERG, M.S. (1978). Cell-cell recognition in multicellular assembly: levels of specificity. In *Cell-Cell Recognition* (Ed. A. Curtis). Symposia of the Society for Experimental Biology no. 32, Cambridge University Press, Cambridge, pp. 25-49.

TOWNES, P.L. and HOLTFRETER, J. (1955). Directed movements and selective adhesion of embryonic amphibian cells. *J. Exp. Zool. 128:* 53-120.

YAMANAKA, H. and EGUCHI, G. (1981). Regeneration of the cornea in adult newts: overall process and behavior of the epithelial cells. *Differentiation 19:* 84-92.